Prolific S-layer shedding and associated proteins from the methanotroph *Methylomicrobium album* BG8

Running title: S-layer of *Methylomicrobium album* BG8

Mariah K. Hermary[a,*], Maria C. Rodriguez Gallo[a], Rachael Rieberger[a], Aurelija M. Grigonyte[b], Kieran McDonald[b], R. Glen Uhrig[a], Dominic Sauvageau[b], and Lisa Y. Stein[a#]

[a]Department of Biological Sciences, University of Alberta, Edmonton AB Canada T6G 2E9

[b]Department of Chemical and Materials Engineering, University of Alberta, Edmonton AB Canada T6H 1H9

*Current Address: Alberta Agriculture and Irrigation, Government of Alberta, Edmonton AB T6H 4P2

#Corresponding Author: CW 405 Bio Sci Bldg, lisa.stein@ualberta.ca

Abstract. Some methanotrophs synthesize S-layers that overlay their outer membrane. TEM imaging revealed that *Methylomicrobium album* BG8 constitutively sheds abundant S-layer units, a phenotype not found in 7 other methanotrophs, even though *Methylotuvimicrobium buryatense* 5GB1 produces a similar structure. Release of S-layer units occurred regardless of carbon (methane or methanol) or nitrogen (ammonium or nitrate) source, with 50X trace metals, under copper deprivation, and at all growth phases. The released S-layer units were isolated from the culture medium of *M. album* BG8 by density gradient centrifugation for proteome analysis. The proteome revealed the S-layer protein subunits, transporters for calcium uptake including TolC and Repeats-in-Toxin (RTX) proteins, transporters for uptake for cobalamin and siderophores, cell wall biogenesis proteins, and proteins with Type I secretion system (T1SS) target domains. *M. album* BG8 adapted to grow at pH 4 lost its S-layer and genome analysis revealed a frameshift mutation plus reduced expression of the S-layer unit gene plus the deletion and almost no expression of an S-layer-associated porin gene. Together, the results suggest that the biogenesis and secretion of *M. album* BG8 S-layer is mediated by its associated T1SS, the S-layer possesses metal acquisition functions, and low pH adaptation of *M. album* BG8 results in loss of S-layer, likely due to reduced, or incomplete, expression of S-layer units and loss of an associated porin. The involvement of the T1SS and shedding phenotype of the S-layer in *M. album* BG8 could be applied towards selective secretion of proteins and other factors of bioindustrial interest.

Importance. The methanotrophic bacterium *M. album* BG8 produces and sheds large quantities of S-layer units into the culture medium regardless of carbon or nitrogen source, metal availability or growth phase. Of the 8 methanotrophic bacteria screened, only

M. album BG8 possessed this phenotype. Proteomics analysis of density gradient purified culture supernatant identified the S-layer protein units and proteins involved in metal uptake and S-layer biogenesis, some with secretion signals for the T1SS. *M. album* BG8 adapted to grow at low pH lost production of its S-layer due to mutations in the genes encoding S-layer units and an associated porin. Better understanding of *M. album* BG8 S-layer production and its shedding phenotype could be harnessed for exporting expressed proteins and bioproducts of industrial interest for ease of collection and downstream processing.

Introduction

Aerobic methanotrophic bacteria are clustered within the Gammaproteobacteria, Alphaproteobacteria and Verrucomicrobia phyla and are metabolically differentiated by their discrete pathways of carbon assimilation (1). Collectively, methanotrophs are of industrial interest for their capacity to convert methane, a potent greenhouse gas, into valuable molecules, from biopolymers to proteins to biofuels (2, 3). The Gammaproteobacterium *Methylomicrobium album* BG8 is a high priority strain for industrialization due to its metabolic flexibility for rapid growth on methane or methanol, with nitrate or ammonium as its nitrogen source (4, 5), and availability of a well-curated genome-scale metabolic model (6). Development of methanotrophs as industrial chassis relies on their ability to express materials of commercial interest at scale, requiring optimization of biomass production and possibly engineering strains to secrete valuable metabolites for ease of downstream processing (3). The diversity of substrates secreted by Type 1 secretion systems (T1SS) makes this system attractive for production and

63 extracellular collection of heterologous proteins, biologics (e.g. growth factors), biosensors,
64 and other molecules (7). Methanotrophs with an active T1SS could potentially be
65 engineered to consume methane for the synthesis and secretion of valuable products that
66 promote biodegradation, metal-scavenging, plant growth, and more, enabling simultaneous
67 greenhouse gas removal and its valorization.

68 Structural analysis of methanotroph cell surfaces has revealed that some strains
69 possess unique S-layers comprised of tightly packed cup-shaped protein units with p6
70 hexagonal symmetry (8-11). It was hypothesized that these structures could provide
71 rigidity to the cell wall and play a role in osmoregulation and tolerance to extremes of
72 salinity and alkalinity (11). A recent study of S-layers from two alkaliphilic
73 *Methylotuvimicrobium* strains validated this hypothesis (12). However, non-halotolerant
74 and neutralophilic methanotrophs, such as *Methylomicrobium album* BG8 (13) and
75 *Methylomicrobium* sp. HG-1 (14), express similar arrays of these cup-like structures on
76 their surfaces, which brings their physiological role and mechanism of biogenesis into
77 question. *Caulobacter crescentus* forms similarly structured S-layers from cup-shaped RsaA
78 proteins with p6 symmetry (15). These RsaA proteins are secreted through a T1SS and
79 contain a span of six repeat-in-toxin (RTX) domains that bind calcium to enable proper
80 folding and stabilization of the crystalline S-layer lattice on the outer membrane (16).
81 Mutations in the N-terminus membrane attachment site of the RsaA protein results in a
82 prolific shedding phenotype (17). Comparison of the *M. album* BG8 RsaA homolog to that of
83 the methanotrophs *Methylotuvimicrobium buryatense* 5GB1 and *Methylotuvimicrobium*
84 *alcaliphilum* 20Z showed only ca. 20% sequence similarity (12). However, all three

methanotroph genomes possess a complete T1SS operon along with their RsaA gene, suggesting that S-layer biogenesis relies on the T1SS similar to that of *C. crescentus.*

The present study shows that *M. album* BG8 constitutively sheds its cup-shaped S-layer units under a variety of nutrient conditions. The cup-shaped S-layer units from the supernatant of *M. album* BG8 cultures were purified using density gradient centrifugation, and proteomic analysis by LC-MS/MS was performed. *M. album* BG8 was adapted to grow at acidic pH, which caused the loss of its S-layer altogether. The observations from this study provide understanding of the morphology, biogenesis, and associated protein functions for released S-layer units of *M. album* BG8, including involvement of a T1SS and calcium binding, plus its complete loss when challenged with growth at low pH. Insights into the biogenesis of S-layer protein units and their prolific release can be used as tools in the production and secretion of valuable industrial proteins using single-carbon molecules as feedstocks.

Results

M. album BG8 constitutively releases abundant cup-shaped S-layer units.

Transmission electron microscopy of *M. album* BG8 displayed cup-shaped particles (Fig. 1) with diameters ranging from 49.5 to 75.2 nm, with an average of 60.9 ± 5.7 nm (n=50; Supp. Table S1). Released S-layer units were observed when *M. album* BG8 was grown in NMS or AMS media containing methane or methanol as a sole carbon source, media devoid of copper, and media containing 50X trace elements solution (examples of TEM images for various conditions are shown in Fig.1). Thus, release of S-layer protein units was considered constitutive, as it did not vary with changes in carbon source, nitrogen source,

108 or metal availability. Released S-layer protein units were also present immediately after
109 culture inoculation, in mid-log growth and at stationary phase (images not shown).
110 However, released S-layer protein units were not detected in the medium of 7 other
111 methanotrophic strains examined (Fig. 2), including cultures of *Methylotuvimicrobium*
112 *buryatense* 5GB1, which possess similar cup-shaped S-layer lattices on its cell surface (11).

113 **S-layer unit proteome suggests associated functions of T1SS, calcium uptake,**
114 **metal acquisition, and membrane assembly.** From the total of 310 peptides identified by
115 LC-MS/MS from purified S-layer units released into the medium of *M. album* BG8 cultures
116 (Supp. Table S2), 14 had high statistical significance across triplicate samples (ranking PSM
117 >4, peptides >5, and score>20). Of note were the S-layer protein itself (H8GFV3), proteins
118 related to binding and uptake of calcium and S-layer assembly (Ca^2 -binding RTX protein,
119 PtrC metalloprotease, pre-pilin N-terminal cleavage) (16, 18, 19), proteins for siderophore
120 and divalent cation uptake (TonB receptor) and cobalamin transport (OM receptor), a
121 porin protein (H8GGQ6), a protein with a T1SS C-terminal target domain (H8GIF1), and a
122 LPS-assembly protein (Table 1, Fig. 3).

123 Proteins with relevance to S-layer biogenesis, but with lower statistical significance
124 (PSM $\leq$5, peptides $\leq$5, score $\leq$20), included TolC, which is the outer-membrane channel
125 component of the T1SS that interacts with the Ca^{2+} binding domains of RTX proteins for
126 their secretion (Table 2) (20). Several membrane-related proteins with lower statistical
127 significance included a cation diffusion facilitator protein, a general secretion pathway
128 "protein D", and TolB from the Tol-Pal system that may have been surreptitiously attached
129 to the released S-layer proteins units. OmpA protein, also associated with the S-layer
130 proteins, may play a role in S-layer biogenesis or tethering to the cell wall as it is an

131 abundant and vital protein in the outer membrane of Gram negative bacteria (21). CorA, a
132 protein once thought to anchor S-layer proteins to the cell wall (10), was only found in one
133 of the triplicate proteome samples at low peptide counts. High counts of flagella-related
134 proteins were co-purified, likely as contaminants from the culture supernatant.

135 Homologs of significantly identified proteins from the proteome were searched for
136 in the genomes of the four gammaproteobacterial methanotrophs screened in this study.
137 Only *M. buryatense* 5GB1 encoded the T1SS gene cluster that includes a homolog of the
138 RsaA S-layer protein (Accession: H8GFV0-H8GFV3); this was expected as this was the only
139 other methanotroph we included that has a S-layer similar to that of *M. album* BG8 (12)
140 (Fig. 3). Although not expressed in the supernatant proteome, a second gene cluster –
141 encoding T1SS ATPase, T1SS HylD membrane fusion protein, a response regulator, and a
142 dihydropteroate synthase (Accession: H8GIU2-H8GIU5) – was identified along with a
143 nearby gene for T1SS TolC (Accession: H8GR48). Sequences of these genes in other
144 methanotrophs showed varying percentages of sequence identity to the genes from *M.*
145 *album* BG8 (Fig. 3).

146 **Loss of S-layer in a strain of *M. album* BG8 adapted to grow at low pH**. To test
147 whether growth at acidic pH had a destabilizing effect on S-layer biogenesis and shedding,
148 as has been shown in *Caulobacter crescentus* (17), we conducted adaptive laboratory
149 evolution on *M. album* BG8 to grow in media from pH 6.8 to 4. Successive transfers in
150 acidified NMS medium resulted in three separate lineages of low pH-adapted cultures. TEM
151 images of the adapted cultures grown on methane or methanol showed smooth cell
152 surfaces devoid of S-layer and the absence of shed S-layer particles into their culture
153 medium (Fig. 4). Genome sequences between the low pH-adapted and parental

154 (unadapted) *M. album* BG8 strains were compared. A frameshift mutation in the S-layer-
155 encoding gene (Metal_0880) at nucleotide 2987/12111, with a Leu substitution at amino
156 acid 996/4036, was identified (Supp. Data, Table 3). Transcriptomic analysis showed that
157 expression of the Metal_0880 gene and its associated T1SS genes (Metal_0877-0879) (12)
158 was ca. 50% lower in the low pH-adapted than in the parental *M. album* BG8 grown in NMS
159 medium at pH 6.8 (Table 3) (5). A frameshift mutation in the gene for a highly expressed
160 porin protein (H8GGQ6) in the S-layer proteome was also identified (Metal_2279), and its
161 transcription was nearly abolished in the low pH-adapted compared to the parental strain
162 (Table 3). These two mutations alone may have resulted in the smooth phenotype of the
163 low pH-adapted strain due to incomplete S-layer unit expression and stabilization or
164 anchoring of S-layer units to the cell wall by the H8GGQ6 porin protein. Thus, adapting *M.*
165 *album* BG8 to grow at low pH resulted in mutations relevant to S-layer biogenesis, yielding
166 complete loss of its S-layer (Fig. 4). No difference in growth rate was detected between the
167 low pH-adapted and parental *M. album* BG8 strains when cultivated in NMS medium at pH
168 6.8 (Supp. Fig. S1). Only the low pH-adapted strains could grow in NMS medium at pH 4,
169 albeit at a slower growth rate than at pH 6.8 (Supp. Fig. S1). The results suggest that the
170 energetic cost of S-layer production did not affect the growth rate of *M. album* BG8 in
171 neutral pH media and that the low pH adaptation process resulted in loss of its S-layer.
172

173 **Discussion**

174 *M. album* BG8 was initially isolated by Roger Whittenbury in 1971 and has been
175 continuously maintained in culture ever since (22). It is likely that the dissociation of its S-
176 layer observed here was acquired by random mutation over the thousands of generations

177 that occurred in laboratory cultures and not a natural feature of the original isolate.
178 Analysis of dissociated S-layer units offers the opportunity to understand more about the S-
179 layer structure, its biogenesis, and its purpose in *M. album* BG8; and provides a basis for the
180 potential utilization of the shedding phenotype to produce and collect products of
181 industrial interest. Based on the most abundant proteins with annotated functions in the
182 proteome of released *M. album* BG8 S-layer units, its biogenesis appears to involve calcium-
183 mediated secretion of S-layer proteins via Ca^{2+}-binding RTX domains of the associated T1SS
184 (19, 20) and assembly with assistance of several outer membrane and other RTX-domain
185 proteins (18, 19), including anchoring to the cell wall by highly expressed porin or other
186 outer membrane proteins (23). The T1SS has three components: an ABC transporter
187 located within the inner membrane, a membrane fusion protein that spans the periplasmic
188 space, and an outer membrane porin protein to create an ATP-dependent translocation
189 mechanism (20). TolC, a highly represented protein in the *M. album* BG8 S-layer unit
190 proteome, forms the outer membrane porin component of the T1SS and transports Ca^{2+}-
191 binding proteins via a Ca^{2+} ratcheting mechanism (20). The protein targets of the T1SS are
192 typically defined by several blocks of nonapeptide-binding consensus sequences located at
193 their C-termini (24). The identification of significant RTX exoprotein and T1SS C-terminal
194 target domain protein in the S-layer unit proteome suggests these T1SS-secreted proteins
195 are associated with the S-layer structure. The significant presence of associated PrtC
196 metalloprotease suggests a putative role in S-layer biogenesis or maintenance, analogous to
197 what is observed with the Sap metalloprotease of *C. crescentus* (25).
198 The S-layer protein (H8GFV3) of *M. album* BG8 is 4,036 amino acids long and
199 contains a conserved hemolysin-type (RTX) calcium-binding region (IPR018511) (19) and

200 a CalX-like domain (IPR038081), with only 35% amino acid identity to the S-layer protein
201 identified in *M. buryatense* 5GB1 (Fig. 3). S-layer proteins are known to display broad
202 diversity between species (26) and the amino acid identity observed between the
203 sequences of S-layer proteins from *M. album* BG8 and *M. buryatense* 5GB1 is above the
204 typical threshold required to consider shared functions (27). In addition, similarly to what
205 is found in *M. album* BG8, a Ca^{+} binding domain was identified in the RsaA S-layer protein of
206 *C. crescentus* (15). Other Gammaproteobacteria that encode homologues to the H8GFV3 S-
207 layer protein of *M. album* BG8 include the close relative *Methylomicrobium lacus* (49% AA
208 ID) and several strains of *Marinobacterium georgiense* (36-37% AA ID)(Supp. Table S2) for
209 which S-layers and membrane blebs have been reported (28). The S-layer proteins of *M.*
210 *album* BG8, *M. buryatense* 5GB1 and *M. alcaliphilum* 20Z are encoded in gene clusters along
211 with cognate T1SS proteins (H8GF0, H8GF1, H8GF2) (29). Here, we showed congruent
212 expression of the three T1SS and S-layer protein genes in both the low pH-adapted and
213 parental strains of *M. album* BG8 through transcriptomic analysis (Table 3), suggesting co-
214 regulation of this gene cluster. Exposure of *C. cresentus* to low pH causes release of its S-
215 layer, which has been used to collect S-layer particles for deeper analysis (25). For *M.*
216 *album* BG8, the S-layer was already actively dissociating from the cell at neutral pH, and
217 further adaptation to low pH resulted in complete loss of S-layer, likely due to a frameshift
218 mutation in the S-layer-encoding gene and a deletion of an S-layer-associated porin gene
219 (Table 3).

220 The copper regulated CorA and CorB proteins of *M. album* BG8 possess Ca^{2+} binding
221 channels (30, 31), and in conjunction with the TonB-ExbB-ExbD transporter system, they
222 can mediate copper and divalent cation uptake and ion homeostasis (30). Correspondingly,

223 two of the proteins with high counts in the S-layer unit proteome were the TonB
224 siderophore receptor protein (H8GGW0) and a Ca^{2+} binding protein (H8GKK7). However,
225 CorA was only found with low counts in one proteome replicate (Supp. Table S2). Although
226 CorA was once considered as a possible anchor point for S-layer proteins (10), a recent
227 study on S-layer of *M. buryatense* 5GB1 showed that its deletion did not affect S-layer
228 production or attachment but did affect copper uptake (12). As neither copper starvation
229 nor growth in 50X trace element solution changed the pattern of S-layer production and
230 release in *M. album* BG8, the shedding phenotype does not appear to be regulated by the
231 abundance of trace metals. Alternatively, the highly expressed porin protein (H8GGQ6)
232 that contained a deletion in the low pH-adapted *M. album* BG8, or the outer membrane
233 beta-barrel domain protein (H8GKR0), could be investigated as potential cell wall anchors
234 similarly to the porin-like proteins of *Deinococcus radiodurans* (23). It is also possible that
235 the LPS assembly protein (H8GJI6) could be a linkage of S-layer to the cell wall in a calcium-
236 dependent fashion similar that of *C. crescentus* (32).
237 Although S-layers can be produced by various methanotrophs, *M. album* BG8 was
238 the only one out of 8 examined from both Alpha- and Gammaproteobacteria to prolifically
239 release S-layer units into the culture. Structures in TEM images surrounding
240 methanotrophs other than *M. album* BG8 included white patches from the phosphotungistic
241 acid negative stain (Fig. 2), membrane protrusions around the surface of *M. oleiharenae*
242 XLMV4^{T} cells (Fig. 2e) (33), sparse spherical particles around some *M. buryatense* 5GB1
243 cells (Fig. 2f), and capsule layer surrounding *M. capsulatus* Bath (Fig. 2g) (22) . None of
244 these structures resembled the released S-layer proteins of *M. album* BG8, but the patchy

245 occurrence of S-layers and capsules among the methanotrophic bacteria continues to be an
246 intriguing topic for future study.

247 **Application of the T1SS and released S-layer proteins for bioindustrial protein**
248 **production.** The industrialization of methanotrophs has been growing in appeal due to the
249 potential to convert methane, a potent greenhouse gas and cheap feedstock, into value-
250 added products such as small metabolites, biofuel precursors, biopolymers, and proteins
251 (34). The phenotype of *M. album* BG8 wherein its S-layer units are delivered from the
252 cytoplasm to the cell surface by the T1SS (35) and then released to the external
253 environment, represents an advantageous protein-production platform. Using the shedding
254 S-layer system, different strategies can be targeted: a heterologous protein can be fused to
255 residues used for excretion through the T1SS for expression of single protein molecules, or
256 the protein of interest can be fused to the N-terminal of the S-layer protein (36) to produce
257 functionalized S-layer units within the culture medium. Of course, the success of such
258 strategies is dependent on the structure and function of the protein of interest but, in each
259 case, the recovery of a heterologous product may be facilitated by the excretion and release
260 mechanism of S-layer units, greatly simplifying downstream processing and reducing
261 associated costs.

262 **Conclusion.** This study identified and characterized the S-layer shedding phenotype
263 of *M. album* BG8 that is not shared by 7 other screened methanotrophic strains. The prolific
264 production and release of *M. album* BG8 S-layer units into the culture medium – likely a
265 consequence of long-term cultivation of this strain – allowed for their purification and
266 proteomic analysis. We identified co-expression of the S-layer protein gene with its
267 neighboring T1SS genes, and in the proteome, we observed the S-layer units, TolC proteins,

268 proteins with T1SS signal sequences, metal-acquisition and membrane biogenesis proteins,
269 and a prominent porin. *M. album* BG8 adapted to grow at low pH through adaptive
270 laboratory evolution acquired mutations in genes encoding S-layer protein and the
271 prominent porin, resulting in low or abolished expression, respectively. These two
272 mutations may be responsible for the constitutive loss of S-layer in the low pH-adapted
273 strain. In *C. crescentus*, S-layer proteins comprise up to 30% to total cellular protein, and
274 considerable energy is required to generate and release S-layer proteins. Yet, *M. album*
275 BG8 grows efficiently and rapidly on both methane and methanol, with a relatively high
276 growth rate compared to other methanotrophs despite its constitutive production and
277 shedding of S-layer (4). The S-layer production and shedding phenotype of *M. album* BG8
278 presents an opportunity to produce and secrete bioproducts of industrial interest including
279 heterologous proteins, growth factors, and metal-chelating agents, among others. Although
280 the cellular energy demands for constitutive S-layer production are high, an added benefit
281 with using *M. album* BG8 is that increased methane consumption will foster optimized
282 rates and yields of bioproduction, which can also yield a larger net climate benefit.
283

284 **Materials and Methods**

285 **Culturing conditions and media**. Eight methanotroph strains maintained in the
286 laboratory were used: Gammaproteobacteria - *Methylomicrobium album* BG8,
287 *Methylomonas denitrificans* FJG1, *Methylicorpusculum oleiharenae* XLMV4T, *Methylococcus*
288 *capsulatus* Bath and *Methylotuvimicrobium buryatense* 5GB1; Alphaproteobacteria -
289 *Methylocystis* sp. WRRC1, *Methylocystis* sp. Rockwell, and *Methylosinus trichosporium* OB3b.
290 Methanotrophs were cultivated in 250-mL Wheaton bottles fitted with screw cap lids inlaid

291 with a butyl rubber septum filled with 100 mL of nitrate (NMS) or ammonium mineral salts
292 (AMS) medium (4), or NMS2 medium (37) for *M. buryatense* 5GB1. Gas headspace (50 mL)
293 was removed from each bottle after which methane (60 mL) was injected via syringe fitted
294 with a 0.22-µm filter. For *M. album* BG8 grown on methanol, 100 µL of high-performance
295 liquid chromatography grade methanol (Sigma-Aldrich) was added. Experiments with
296 increased trace metals included 50X standard trace element solution. Experiments with
297 copper-free media included Chelex 100 (BioRad)-treated media (except the trace-elements
298 solution) added to acid-washed Wheaton bottles. 1 mL (1%) inoculum from a late
299 exponential phase culture that had been passaged at least once under the identical growth
300 conditions for each experimental condition was used for each strain. Cultures were
301 incubated at 30°C, with the exception of 37°C for *M. capsulatus* Bath, with shaking at 150
302 rpm until early stationary phase as determined by growth curves (OD_{540}) (4).

303 **Adaptation of *M. album* BG8 to low pH and analysis of genome-wide mutations**.
304 A series of NMS medium formulations from pH 6.8 to 3.8 in 0.2 pH unit increments were
305 generated using mixtures of KH_2PO_4, Na_2HPO_4 and citrate phosphate buffers with further
306 acidification by dropwise addition of 0.1 M HCl to achieve the desired final pH prior to
307 autoclaving. Cultures were grown on methane/air (30/70%) and passaged a minimum of
308 three times before moving to the next lower pH medium. Adaptation experiments were
309 performed from 2022-2024. Visualization of the adapted cells was performed by TEM as
310 described below. Genomic DNA was extracted from three replicated culture lines from
311 parental (non-adapted) and pH 4-adapted *M. album* BG8 grown on NMS medium at pH 6.8
312 using the DNeasy Blood and Tissue Kit (Qiagen), cleaned using the ZymoDNA clean and
313 concentrator kit (Zymo Research, USA) and measured by the Qubit dsDNA broad range

314 assay (Fisher Scientific, USA). Genomes were sequenced using Ilumina Novoseq (Genome
315 Quebec, Montreal) with 1060X (adapted) and 1173X coverage. The adapted genome was
316 aligned to the parental genome using SPAdes (v4.2.0+galaxy0). Snippy (v4.6.0+galaxy0)
317 was used to identify mutations in the consensus adapted genome.

318 **Transmission electron microscopy imaging**. Cells (ca. 2 mL) were removed from
319 cultures and pelleted by centrifugation (5 min at 6000 x *g*; Eppendorf). Cell pellets were
320 rinsed and resuspended in 500 µL phosphate buffer. Cell samples were placed on a 300-nm
321 copper grid for 4 to 6 min prior to staining with 1% phosphotungistic acid. Images were
322 captured using a Philips/FEI Transmission Electron Microscope with Gatan Camera
323 (Morgagni). Fig. 2 was imaged with a JEOL JEM-ARM200CF S/TEM electron microscope at
324 an accelerating voltage of 200 kV. The HAADF-STEM images were collected with the JEOL
325 HAADF detector using the following experimental conditions: probe size 6C, condenser
326 lens aperture 30 µm, scan speed 32 µs per pixel, and camera length 8 cm. The average
327 diameter of S-layer proteins starting from the outer edge were measured using ImageJ
328 (n=50).

329 **S-layer purification.** Three technical replicates were used for purification and LC
330 MS/MS proteomics with each replicate deriving from 1 L of *M. album* BG8 culture grown in
331 NMS medium with methane. The purification method is illustrated in Fig. 5, and was
332 adapted from a protocol for isolation of outer membrane vesicles (38). For each replicate,
333 the cultures were filtered using a 0.45-µm PES stericup (Millipore) to separate biomass
334 from filtrate containing the S-layer proteins. The filtrate was passed through a 100 kDa MW
335 cutoff protein concentrator (GE Vivaspin) and retentate was collected by rinsing the filter

336 with 1 mL phosphate buffer at pH 6.8. Retentate aliquots were spotted on NMS agar and
337 incubated with methane to confirm the absence of viable *M. album* BG8 cells.
338 The crude retentate was mixed with OptiPrep (iodixanol; Sigma-Aldrich) (60%) and
339 placed at the bottom of a sterile centrifuge tube. A discontinuous density gradient was
340 created by layering 2 mL of diluted OptiPrep (40, 35, 30, 25, 20% using OptiPrep Diluent)
341 as per manufacturer's instructions. Samples were centrifuged for 12 h at 53,000 rpm
342 (~288,350 x *g*) at 4°C in a Ti70 Fixed rotor ultracentrifuge (Beckman Optima L-90K
343 Ultracentrifuge). 1-mL fractions were removed by pipetting from the top of the density
344 gradient, with a total of 18 fractions per replicate. Each fraction was measured for
345 refractive index (Reichert AR200 Automatic Digital Refractometer) to ensure that the
346 density gradient was maintained. Per fraction, 50 µL was denatured using 50 µL of 2x
347 Laemmli Sample Buffer (BioRad) and incubation on a heat block (Baxter Canlab H2025-1
348 Dry Block Heater) at 95°C for 5 min. The prepared samples were separated on an 8%
349 acrylamide gel and stained with colloidal Coomassie to determine protein presence.
350 Protein-containing fractions were denatured and concentrated using a protein centrifuge
351 concentrator (Amicon) to a final volume of 50 µL. Concentrated protein samples were
352 partially resolved through a precast 4-20% acrylamide gradient gel (BioRad) to remove the
353 Optiprep solvent until no residual sample was present in the wells of the gel. Protein
354 samples were excised from the gel and submitted for LC-MS/MS analysis.
355 **In-Gel Digest of S-layer Peptides.** The gel bands were cut into small pieces and
356 destained four times with 50% Acetonitrile (ACN; Sigma) in 50 mM trietylammonium
357 bicarbonate (TEAB; Sigma) at 37°C for 10 min. Destained gel pieces were washed with 100
358 mM TEAB at 37°C for 10 min and dehydrated by incubating them twice in 100 % ACN at

359 room temperature for 10 min to complete drying. Cysteine residues were reduced by
360 incubating dried gel slices in 10 mM dithiothreitol (DTT; BioRad) solution in 100 mM
361 TEAB for 45 min at 37°C. Reduction solution was replaced with 55 mM iodoacetamide (IA;
362 Sigma) in 100 mM TEAB buffer and incubated in the dark for 1 h at 37°C to alkylate
363 cysteine residues. The alkylation solution was replaced by 100 mM TEAB and incubated
364 for 10 min, repeated twice. Gel pieces were then dehydrated once more in 100% ACN and
365 dried as stated above. Gel pieces were rehydrated by adding 6 ng/µL trypsin (Promega;
366 V5113) in 100 mM TEAB. Peptides were digested for 16 h at 37 °C with shaking at 150
367 rpm. Tryptic peptides were retained, and in-gel digested peptides were further extracted
368 by incubating in 1% (v/v) formic acid (FA; Fisher), 2% (v/v) ACN in 100 mM TEAB for 1 h
369 at 37°C. This was followed by a second 1 h 37°C extraction using a 1:1 1% (v/v) FA in 100
370 mM TEAB and 100% ACN extraction buffer. Digested peptide fractions were pooled and
371 dried. Isolated peptides were re-suspended and desalted using ZipTip C18 pipette tips
372 (ZTC18S960; Millipore), as described (39). All peptides were dried and re-suspended in 3%
373 (v/v) ACN / 0.1% (v/v) FA immediately prior to mass spectrometry analysis.
374 **Liquid chromatography mass spectrometry.** Re-suspended tryptic peptides were
375 analyzed using nano flow HPLC (Easy-nLC 1000, Thermo Scientific) with an EASY-Spray
376 capillary HPLC column (PepMap RSLC C18, 75um x 25cm, 100Å, 2µm, Thermo Scientific)
377 coupled to a Q Exactive Orbitrap mass spectrometer (Thermo Scientific). Dissolved samples
378 were injected using an Easy-nLC 1000 system (Thermo Scientific). The column was
379 equilibrated with 100% solvent A (0.1% (v/v) FA, 4% (v/v) ACN in water). Peptides were
380 eluted using the following gradient of solvent B (0.1% (v/v) FA in 80% (v/v) ACN): 0–18%
381 B, 0–73 min; 18–30% B, 73-101 min; 30–46% B, 101–120 min; 46–100% B, 120-123, min

382 at a flow rate of 0.35 µl min−1 at 50°C. High-accuracy mass spectra were acquired in data-
383 dependent acquisition mode. All precursor signals were recorded in a mass range of 300–
384 1,700 m/z and a resolution of 35,000 at 200 m/z. The maximum accumulation time for a
385 target value of 1×10^6 was set to 120 ms. Up to 12 data-dependent MS/MS were recorded
386 using quadrupole isolation with a window of 2 Da and higher-energy collisional
387 dissociation fragmentation with 26% fragmentation energy. A target value of 5×10^4 was
388 set for MS/MS using a maximum injection time of 250 ms and a resolution of 17,500 at 200
389 m/z. Precursor signals were selected for fragmentation with charge states from +2 to +7
390 and a signal intensity of at least 1×10^4. All precursor signals selected for MS/MS were
391 dynamically excluded for 30s.

392 All acquired mass spectrometry data was analyzed using Proteome Discoverer (ver.
393 2.4.1.15). Data were searched against the *M. album* BG8 proteome (UNIPROT
394 H8GRI8_METAL; containing 3,738 protein sequences) using an automatically generated
395 decoy database and the Proteome Discoverer processing workflow
396 (PWF_QE_Basic_SeaquestHT) and consensus workflow (CWF_Basic) with minimal
397 deviation. Deviations included: a precursor and fragment mass tolerance of 10 ppm and 0.6
398 da, respectively, trypsin digestion with 2 missed cleavages, variable modifications
399 methionine oxidation (+15.995 Da), n-terminal acetylation (+42.011 Da), methionine loss (-
400 131.040 Da), methionine loss + n-terminal acetylation (-89.030 Da) and fixed modifications
401 carbamidomethylation (+57.021 Da).

402 **Identifying similar protein sequences in other methanotrophs.** To determine if
403 identified S-layer-associated proteins were unique to *M. album* BG8, each identified protein
404 sequence was compared using BLASTp to the gammaproteobacterial methanotrophs:

Methylomonas denitrificans FJG1 (taxon:416); *Methylicorpusculum oleiharenae* XLMV4T (taxon:1338687); *Methylotuvimicrobium buryatense* 5GB1 (taxon:1338687); and *Methylococcus capsulatus* Bath (taxon:414). (https://blast.ncbi.nlm.nih.gov/). The presence of T1SS proteins identified in the *M. album* BG8 genome (GenBank: CM001475.1) were also analyzed for their presence in the above gammaproteobacterial genomes. For query sequences with a high number of BLASTp hits, only matches with the highest percent identities to the query were reported.

To determine the presence of S-layer related proteins in gammaproteobacterial methanotrophs that were not analyzed in this experiment, the proteins of interest were screened against the entire *Methylococcaceae* group (taxid:135618) using BLASTp (Supp. Table S3). The S-layer protein H8GFV3 was further screened via BLASTp against all Gammaproteobacteria (taxid:1236) (Supp. Table S4).

RNA extraction and RNAseq analysis. Total RNA was extracted from triplicate late-log phase cultures of the low-pH adapted *M. album* BG8 grown in NMS medium at pH 6.8 (Supp. Fig. S1) using the QIAWave RNA Mini Kit (Qiagen) following the manufacturer's protocol. The extracted RNA was quantified using the Qubit RNA high sensitivity assay (Fisher Scientific, USA) and quality controlled using the Agilent 2100 Bioanalyzer. RNA libraries were prepared by Genome Quebec (Montreal, Canada) using a bacterial rRNA-depleted RNA-seq library preparation workflow, followed by sequencing on an Illumina NovaSeq (PE100, ~25 M reads per sample, ±5 M). Raw paired-end RNAseq reads were analyzed using the Galaxy web platform (usegalaxy.eu; version 25.0). First, reads were quality filtered using Trimmomatic (v0.39+galaxy2) with default parameters. High-quality reads were mapped to the low-pH adapted *M. album* BG8_1aa genome using HISAT2 (v2.2.1+galaxy0). The number of reads

mapped to each gene was calculated by HTseq-count (v2.0.9+galaxy0) and the output was used to calculate normalized transcript abundances in transcripts per million (TPM). Statistically validated TPM values for the same genes from the parental *M. album* BG8 strain grown in NMS media with methane were used from a prior RNAseq experiment with triplicate samples (5).

Acknowledgments: The authors would like to thank Arlene Oatway and Dr. Kacie Norton from the Biological Sciences Microscopy Unit and Haoyang Yu from NanoFAB with assisting in transmission electron microscopy imaging. All peptide digestion and LC-MS/MS preparation were performed at the Alberta Proteomics and Mass Spectrometry Facility at the Univ. Alberta.

Data availability: All raw proteomics files were submitted to the PRoteomics IDEntification Database (PRIDE; https://www.ebi.ac.uk/pride/). Reviewer access details are as follows: Dataset: PXD050176, Username: reviewer_pxd050176@ebi.ac.uk, Password: pGJMeScS.. The genome and RNAseq data for low pH-adapted *M. album* BG8 grown in NMS at pH 6.8 can be found under Genbank accession number PRJNA698057. Transcriptome data for parental *M. album* BG8 grown in NMS at pH 6.8 can be found under accession Genbank number PRJNA698057. Further information on the genome mutations and calculations of RNAseq TPM values for the low pH-adapted strain are in the Supp. Data Sheet.

Funding statement: This work was supported by NSERC Discovery grants to DS and LYS, Canada First Research Excellence Funds (Future Energy Systems) awarded to DS and LYS,

the Government of Alberta Major Innovation Fund award (RCES) to DS and LYS, and two CFI John Evans Leadership Fund (JELF) awards provided to RGU and DS.

Conflict of interest: the authors have no conflicts of interest to declare.

Author Contributions: **Author Contributions:** M.K.H., D.S. and L.Y.S. conceptualized the research. M.K.H. carried out the experiments and created the figures and tables. R.G.U. and M.C.R.G. provided peptide digestion, LC-MS/MS preparation and corresponding proteome analysis. A.M.G. provided bioinformatics analysis. R.R. performed the pH adaptation experiments, genome sequencing of the parental and adapted strains, and RNAseq analysis. M.K.H., D.S. L.Y.S. wrote the initial version of the manuscript. All authors edited the manuscript. D.S. and L.Y.S. co-supervised the work. All authors have given consent to the final version of the manuscript.

Permission to print information from another source. Figure 5 was an adapted protocol with permission from Microbiological Research.

Originality statement: None of the work in this manuscript has been published or submitted for publication elsewhere.

References:

1. **Khmelenina VN, But SY, Rozova ON, Trotsenko YA.** 2019. Metabolic features of aerobic methanotrophs: news and views. Curr Issues Mol Biol **33:**85–99.
2. **Kang NK, Chau THT, Lee EY.** 2024. Engineered methane biocatalysis: strategies to assimilate methane for chemical production. Curr Op Biotechnol **85:**103031.

3. **Sauvageau D, Stein LY, Arenas E, Das S, Iacobelli M, Lawley M, Lazic M, Rondon FL, Weiblen C.** 2024. Industrializing methanotrophs and other methylotrophic bacteria: from bioengineering to product recovery. Curr Op Biotechnol **88:**103167.
4. **Tays C, Guarnieri MT, Sauvageau D, Stein LY.** 2018. Combined effects of carbon and nitrogen source to optimize growth of proteobacterial methanotrophs. Front Microbiol **9:**2239.
5. **Sugden S, Lazic M, Sauvageau D, Stein LY.** 2021. Transcriptomic and metabolomic responses to carbon and nitrogen sources in *Methylomicrobium album* BG8. Appl Environ Microbiol **87**.
6. **Villada JC, Duran MF, Lim CK, Stein LY, Lee PKH.** 2022. Integrative genome-scale metabolic modeling reveals versatile metabolic strategies for methane itilization in *Methylomicrobium album* BG8. mSystems **7:**e0007322.
7. **Pourhassan ZN, Smits SHJ, Ahn JH, Schmitt L.** 2021. Biotechnological applications of type 1 secretion systems. Biotechnol Adv **53:**107864.
8. **Khmelenina VN, Suzina NE, Trotsenko YA.** 2013. Surface layers of methanotrophic bacteria. Microbiology **82:**529–541.
9. **Trotsenko YA, Khmelenina VN.** 2002. The biology and osmoadaptation of haloalkaliphilie methanotrophs. Microbiology **71:**123–132.
10. **Shchukin VN, Khmelenina VN, Eshinimayev BT, Suzina NE, Trotsenko YA.** 2011. Primary characterization of dominant cell surface proteins of halotolerant methanotroph *Methylomicrobium alcaliphilum* 20Z. Microbiology **80:**608–618.
11. **Khmelenina VN, Shchukin VN, Reshetnikov AS, Mustakhimov, II, Suzina NE, Eshinimaev BT, Trotsenko YA.** 2010. Structural and functional features of methanotrophs from hypersaline and alkaline lakes. Microbiology **79:**472–482.
12. **Hamilton R, Gebbie W, Bowman C, Mantanona A, Kalyuzhnaya MG.** 2025. Microbial hauberks: composition and function of surface layer proteins in gammaproteobacterial methanotrophs. Appl Environ Microbiol **91:**e0136424.
13. **Jeffries P, Wilkinson JF.** 1978. Electron microscopy of cell wall complex of *Methylomonas albus*. Arch Microbiol **119:**227–229.
14. **Kim HG, Han GH, Eom CY, Kim SW.** 2008. Isolation and taxonomic characterization of a novel type I methanotrophic bacterium. J Microbiol **46:**45–50.
15. **Bharat T, Kureisaite-Ciziene, D., Hardy, G. et al.** 2017. Structure of the hexagonal surface layer on Caulobacter crescentus cells. Nat Microbiol **2:**17059.
16. **Herrmann J, Jabbarpour F, Bargar PG, Nomellini JF, Li PN, Lane TJ, Weiss TM, Smit J, Shapiro L, Wakatsuki S.** 2017. Environmental calcium controls alternate physical states of the *Caulobacter* surface layer. Biophys J **112:**1841–1851.
17. **Ford MJ, Nomellini JF, Smit J.** 2007. S-layer anchoring and localization of an S-layer-associated protease in Caulobacter crescentus. J Bacteriol **189:**2226–2237.
18. **Bao K, Claesson R, Gehrig P, Grossmann J, Oscarsson J, Belibasakis GN.** 2022. Proteomic characterization of the oral pathogen *Filifactor alocis* reveals key inter-protein pnteractions of Its RTX toxin: FtxA. Pathogens **11**.
19. **Linhartová I, Bumba L, Mašín J, Basler M, Osička R, Kamanová J, Procházková K, Adkins I, Hejnová-Holubová J, Sadílková L, Morová J, Sebo P.** 2010. RTX proteins: a highly diverse family secreted by a common mechanism. FEMS Microbiol Rev **34:**1076–1112.
20. **Bumba L, Masin J, Macek P, al. e.** 2016. Calcium-Driven Folding of RTX Domain β-Rolls Ratchets Translocation of RTX Proteins through Type I Secretion Ducts. Molec Cell **62:**47–62.
21. **Samsudin F, Ortiz-Suarez ML, Piggot TJ, Bond PJ, Khalid S.** 2016. OmpA: A Flexible Clamp for Bacterial Cell Wall Attachment. Structure **24:**2227–2235.
22. **Whittenbury R, Phillips KC, Wilkinson JF.** 1970. Enrichment, isolation and some properties of methane-utilizing bacteria. J Gen Microbiol **61:**205–218.

23. **von Kügegen A, van Dorst S, Alva V, Bharat T.** 2022. A multidomain connector links the outer membrane and cell wall in phylogenetically deep-branching bacteria. Proc Natl Acad Sci **119**.
24. **Spitz O, Erenburg IN, Beer T, Kanonenberg K, Holland IB, Schmitt L.** 2019. Type I secretion systems-one mechanism for all? Microbiol Spect **7:**10.1128/microbiolspec.psib–0003–2018.
25. **Ford MJ, Nomellini JF, Smit J.** 2007. S-Layer anchoring and localization of an S-Layer-associated protease in *Caulobacter crescentus*. J Bacteriol **189:**2226–2237.
26. **Fagan R, Fairweather N.** 2014. Biogenesis and functions of bacterial S-layers. Nat Microbiol **12:**211–222.
27. **Sander C, Schneider R.** 1991. Database of homology-derived protein structures and the structural meaning of sequence alignment. Proteins **9:**56–68.
28. **González JM, Mayer F, Moran MA, Hodson RE, Whitman WB.** 1997. Microbulbifer hydrolyticus gen. nov., sp. nov., and Marinobacterium georgiense gen. nov., sp. nov., Two Marine Bacteria from a Lignin-Rich Pulp Mill Waste Enrichment Community. Int J Syst Evol Microbiol **47:**369–376.
29. **Hamilton R, Gebbie W, Bowman C, Mantanona A, Kalyuzhnaya MG.** 2024. Microbial Hauberks: Composition and Function of Surface Layer Proteins in Gammaproteobacterial Methanotrophs. bioRxiv doi:https://doi.org/10.1101/2024.07.09.602694
30. **Khmelenina VN, Suzina NE, Trotsenko YA.** 2013. Surface layers of methanotrophic bacteria. Microbiology **82:**529–541.
31. **Johnson KA VT, Larsen Ø, Pedersen RB, Lillehaug JR, Jensen HB, et al.** 2014. CorA is a copper repressible surface-associated copper(I)-binding protein produced in *Methylomicrobium album* BG8. Plos One **9:**e87750.
32. **von Kügelgen A, Tang H, Hardy GG, Kureisaite-Ciziene D, Brun YV, Stansfeld PJ, Robinson CV, Bharat TAM.** 2020. In situ structure of an intact lipopolysaccharide-bound bacterial surface layer. Cell **180:**348–358.e315.
33. **Saidi-Mehrabad A, Kits DK, Kim JJ, Tamas I, Schumann P, Khadka R, Strilets T, Smirnova AV, Rijpstra WIC, Damsté JSS, Dunfield PF.** 2020. *Methylicorpusculum oleiharenae* gen. nov., sp. nov., an aerobic methanotroph isolated from an oil sands tailings pond. Int J Syst Evol Microbiol **70:**2499–2508.
34. **Pham DN, Nguyen AD, Lee EY.** 2022. Outlook on engineering methylotrophs for one-carbon-based industrial biotechnology. Chem Eng J **449**.
35. **Kalyuzhnaya M, Demidenko O, Collins D.** 2018. Compositions and methods using methanotrophic s-layer proteins for expression of heterologous proteins. USA.
36. **Sára M, Sleytr UB.** 2000. S-Layer Proteins. J Bacteriol **182:**859–868.
37. **Puri AW, Owen S, Chu F, Chavkin T, Beck DAC, Kalyuzhnaya MG, Lidstrom ME.** 2015. Genetic tools for the industrially promising methanotroph *Methylomicrobium buryatense*. Appl Environ Microbiol **81:**1775–1781.
38. **Klimentová J, Stulík J.** 2015. Methods of isolation and purification of outer membrane vesicles from gram-negative bacteria. MIcrobiol Res **170:**1–9.
39. **Uhrig RG, Schläpfer P, Roschitzki B, Hirsch-Hoffmann M, Gruissem W.** 2019. Diurnal changes in concerted plant protein phosphorylation and acetylation in Arabidopsis organs and seedlings. Plant J **99:**176–194.

Table 1. Significant peptide hits from LC-MS/MS detection of purified released S-layer protein units (n=3) organized by Genbank locus tag.

Genbank Locus Tag	Uniprot Accession	UniProt Description	Mean PSM	Mean peptide	Mean score	COG Category
Metal_0147	H8GKK7	Ca2+-binding protein, RTX toxin	5.7	5.7	18.5	Secondary metabolites biosynthesis, transport and catabolism
Metal_0479	H8GNA1	Uncharacterized protein (Metallo-protease PrtC*)	30.3	15.7	106.7	Secondary metabolites biosynthesis, transport and catabolism
Metal_0659	H8GPP0	Uncharacterized protein	7	1	20	Inorganic ion transport and metabolism
Metal_0880	**H8GFV3**	**S-layer protein**	**7.3**	**6.3**	**23.2**	**Secondary metabolites biosynthesis, transport and catabolism**
Metal_1116	H8GHU9	Prepilin-type N-terminal cleavage/methylation domain-containing protein	64.3	4	231.4	Intracellular trafficking, secretion, and vesicular transport
Metal_1447	H8GKR0	Outer membrane protein beta-barrel domain-containing protein*	5	2	17.9	Cell wall/membrane/envelope biogenesis
Metal_1728	H8GMU5	Flagellin	331.7	22.3	1316.7	Cell motility
Metal_1783	H8GNF7	Flagellar hook protein FlgE	16	8.7	51.7	Cell motility
Metal_2279	H8GGQ6	Uncharacterized porin	16	4.7	52.5	Cell wall/membrane/envelope biogenesis
Metal_2337	H8GGW0	TonB-dependent siderophore receptor	7	6.3	20.2	Inorganic ion transport and metabolism
Metal_2634	H8GJI6	LPS-assembly protein LptD	16.7	2.7	43.8	Cell wall/membrane/envelope biogenesis
Metal_3768	H8GIA0	ATP synthase epsilon chain	9.7	1	22.4	Lipid transport and metabolism
Metal_3821	H8GIF1	Type I secretion C-terminal target domain protein	24.5^{+}	12.5^{+}	71.9^{+}	Secondary metabolites biosynthesis, transport and catabolism
Metal_3919	H8GJ49	Outer membrane cobalamin receptor protein	8	6.3	22.5	Coenzyme transport and metabolism

*HHpred protein annotation (>95% probability), "+" replicates n=2, bolded protein = major S-layer unit

Table 2. Additional protein hits of interest from LC-MS/MS detection of purified released S-layer protein units organized by Genbank locus tag.

Genbank Locus Tag	UniProt Accession	UniProt Description	Mean PSM	Mean Peptide	Mean Score	COG Category
Metal_0094	H8GK04	Cation diffusion facilitator family transporter	2.5	1.00[b]	6.19	Inorganic ion transport and metabolism
Metal_0482	H8GNA4	Uncharacterized protein	4.67	2	11.77	-
Metal_0879	**H8GFV2**	**Type I secretion outer membrane protein, TolC family**	**3**	**3**	**8.09**	**Cell wall/membrane /envelope biogenesis; Intracellular trafficking, secretion, vesicular tnspt.**
Metal_1031	H8GH59	PAS domain S-box/diguanylate cyclase (GGDEF) domain-containing protein	3.50[a]	1	9.16	Signal transduction mechanisms
Metal_1419	H8GK80	Outer membrane protein/peptidoglycan-associated (Lipo)protein	3	2.33	8.32	Cell wall/membrane /envelope biogenesis
Metal_1666	H8GM80	Autotransporter secretion inner membrane protein TamB	3.33	1	7.05	-
Metal_1730	H8GMU7	Flagellar hook-associated protein 2	5	5	13.49	Cell motility
Metal_1789	H8GNG3	Flagellar hook-associated protein 1	2.67	2.67	8.48	Cell motility
Metal_1790	H8GNG4	Flagellar hook-associated protein 3	2.33	2.33	6.55	Cell motility
Metal_1986	H8GPX1	Citrate lyase beta subunit	2.33	1	8.01[c]	Carbohydrate transport and metabolism
Metal_1998	H8GPY3	Outer membrane protein/peptidoglycan-associated (Lipo)protein	2.67	2.33	7.49	Cell wall/membrane /envelope biogenesis
Metal_2207	H8GG32	Adenosylhomocysteinase	3.33	1.33	4.8	Coenzyme transport and metabolism
Metal_2282	H8GGQ9	DNA-binding transcriptional regulator NtrC	2.67	1	6.79	Signal transduction mechanisms
Metal_2345	H8GGW4	Uncharacterized protein	2.67	1	6.78	Function unknown
Metal_2446	H8GI24	Uncharacterized protein	4.00[a]	1	10.57	-
Metal_2469	H8GI44	PQQ-dependent dehydrogenase, methanol/ethanol family	3	3	7.4	Carbohydrate transport and metabolism
Metal_2481	H8GI56	Uncharacterized protein	2.50[a]	2.5	6.29	-
Metal_2515	H8GI88	Probable cytosol aminopeptidase	2.33	2	6.21	Amino acid transport and metabolism
Metal_2819	H8GL29	Tol-Pal system protein TolB	4.67	4.33	14.22	Intracellular trafficking, secretion, and vesicular transport

Metal_2821	H8GL31	Cell division coordinator CpoB	5	5	11.65	Cell cycle control, cell division, chromosome partitioning
Metal_3055	H8GN21	Uncharacterized protein	4	1	8.92	Function unknown
Metal_3106	H8GNM8	Hemolysin-coregulated protein	3.67	3	10.3	Function unknown
Metal_3255	H8GPH9	Murein lipoprotein	1.67	1.67	6.06	Function unknown
Metal_3338	H8GQ61	Uncharacterized protein	3	2.67	7.27	Function unknown
Metal_3460	H8GRD0	Transaldolase	4.33	4	10.21	Nucleotide transport and metabolism
Metal_3679	H8GHK8	Gly-zipper_OmpA domain-containing protein	3.5	2	12.03[c]	Function unknown
Metal_3822	H8GIF2	VCBS repeat-containing protein	2.67	2	11.46[c]	Secondary metabolites biosynthesis, transport and catabolism
Metal_3828	H8GIF8	General secretion pathway protein D	3	2.5	7.94[c]	Cell motility; Intracellular trafficking, secretion, and vesicular transport

[*] HHpred protein annotation (>95%)
[a] Absent in replicate A
[b] Absent in replicate B
[c] Absent in replicate C

573 **Table 3.** Mutations and level of transcription (Transcripts per million) identified in the
574 genome and RNAseq data of *M. album* BG8 adapted to growth at pH 4. The adapted genome
575 was compared to the parental genome. Gene expression levels in the adapted and parental
576 transcriptomes are reported. The two genes in bold were identified in the S-layer
577 proteome.

Genbank Locus Tag	UniProt Accession	Type of Mutation	UniProt Function	TPM[1] Adapted	TPM[1] Parental
Metal_0463	H8GN86	Synonymous	Serine/threonine protein kinase	105	61
Metal_0492	H8GNB4	Synonymous	Malto-oligosyltrehalose synthase	28	3
Metal_0877	***H8GFV0***	***none***	***Type I secretion system ABC transporter, PrtD family***	***128***	***252***
Metal_0878	***H8GFV1***	***none***	***Type I secretion membrane fusion protein, HlyD family***	***97***	***167***
Metal_0879	***H8GFV2***	***none***	***Type I secretion outer membrane protein, TolC family***	***81***	***181***
Metal_0880	**H8GFV3**	**Frameshift (delT at nt 2987; Leu at aa 996**	**S-layer protein**	**1764**	**3948**
Metal_0915	H8GFY7	Insertion	Drug resistance transporter, EmrB/QacA subfamily	46	67
Metal_0961	H8GGI4	Frameshift	Choline dehydrogenase-like flavoprotein	104	20
Metal_1085	H8GHB2	Synonymous	Ketol-acid reductoisomerase (NADP(+))	449	703
Metal_1113	H8GHU6	Glu – Val	Uncharacterized protein	154	44
Metal_1464	H8GKS7	Asp – Gly	DNA-binding protein H-NS	2960	2618
Metal_1726	H8GMU4	Asp – Ser	Flagellar protein FliL	70	22
Metal_1910	H8GP90	Synonymous	Rhodanese-related sulfurtransferase	56	66
Metal_1927	H8GPA7	Val – Ile	Putative PLP-dependent enzyme possibly involved in cell wall biogenesis	115	96
Metal_2019	H8GQF3	Asp – Asn	Succinate dehydrogenase hydrophobic membrane anchor subunit	135	105
Metal_2096	H8GQM4	Synonymous	Putative thymidine phosphorylase	77	76

Metal_2101	H8GR29	Val – Gly	Probable membrane transporter protein	18	8
Metal_2132	H8GR59	Synonymous	Cadherin domain-containing protein	66	35
Metal_2140	H8GR66	Val – Leu	Protein-export membrane protein SecG	767	1324
Metal_2279	**H8GGQ6**	**inframe deletion**	**Porin**	**21**	**865**
Metal_2323	H8GGU6	Glu – Gly	Cytochrome c	45	58
Metal_2426	H8GHJ6	Deletion	RHS repeat-associated core domain protein	20	5
Metal_2567	H8GIU3	Deletion	Membrane fusion protein (MFP) family protein	132	91
Metal_2569	None**	Insertion	TolC family outer membrane protein	873	428
Metal_2678	H8GJM5	Glu – Ala	Tfp pilus assembly protein PilN	95	48
Metal_2685	H8GJN2	Leu – Pro	C-terminal processing peptidase	215	407
Metal_2779	H8GKZ0	Deletion	Transcriptional regulator	35	40
Metal_3143	H8GNR1	1 missense, 2 synonymous	Transposase	40	40
Metal_3171	H8GNT9	Ser – Asn	Phosphatidylserine decarboxylase proenzyme	72	271
Metal_3777	H8GIA9	Val – Ala	Cobalt-zinc-cadmium resistance protein CzcC	60	53
Metal_3987	H8GJT4	Leu – Pro	Transglutaminase-like domain-containing protein	36	93

578 (1)TPM: mRNA transcripts per million; data was collected for *M. album* BG8 growing in NMS medium at pH 6.8.
579 *mRNA expression values of the three T1SS genes associated with the S-layer structural gene are reported to
580 compare between the low pH adapted and parental strains.
581 ** UniProt accession number not available; protein function supported by InterProScan and blastp
582 annotation.
583
584
585

Figure Legends:

Figure 1. Transmission electron micrographs of *M. album* BG8 with released S-layer protein units (as depicted with arrows) when cultured with methane in various media conditions. (a) NMS media (b) AMS media without copper (c) NMS media with 50X trace elements solution. Micrographs contain a wide range of scales to highlight membrane morphology and adjacent surrounding areas.

Figure 2. Transmission electron micrographs of selected alpha- and gammaproteobacterial methanotrophs cultivated on methane and NMS. (a) *Methylocystis* sp. WRRC1 (b) *Methylocystis* sp. Rockwell (c) *Methylosinus trichosporium* OB3b (d) *Methylomonas denitrificans* FJG1 (e) *Methylicorpusculum oleiharenae* XLMV4^{T} (f) *Methylotuvimicrobium buryatense* 5GB1 (g) *Methylococcus capsulatus* Bath.

Figure 3. Protein sequence comparison of S-layer and T1SS- related proteins of *M. album* BG8 to gammaproteobacterial methanotrophs *M. denitrificans* FJG1, *M. oleiharenae* XLMV4^{T}, *M. buryatense* 5GB1 and *M. capsulatus* Bath.

Figure 4. A) *M. album* BG8 (parental strain, unadapted) grown in NMS at pH 6.8 in methane or methanol showing prolific shedding of S-layer particles and the presence of flagella in the surrounding media. B) *M. album* BG8 adapted to grow at pH 4, cultivated in methane or methanol, showing absence of S-layer particles in the surrounding media. C) Low pH-adapted *M. album* BG8 grown at pH 6.8 in methane or methanol NMS showing continued absence of S-layer particles in the surrounding media.

Figure 5. S-layer isolation and purification protocol based on density gradient centrifugation for *M. album* BG8 adapted from a protocol for OMV isolation (38).

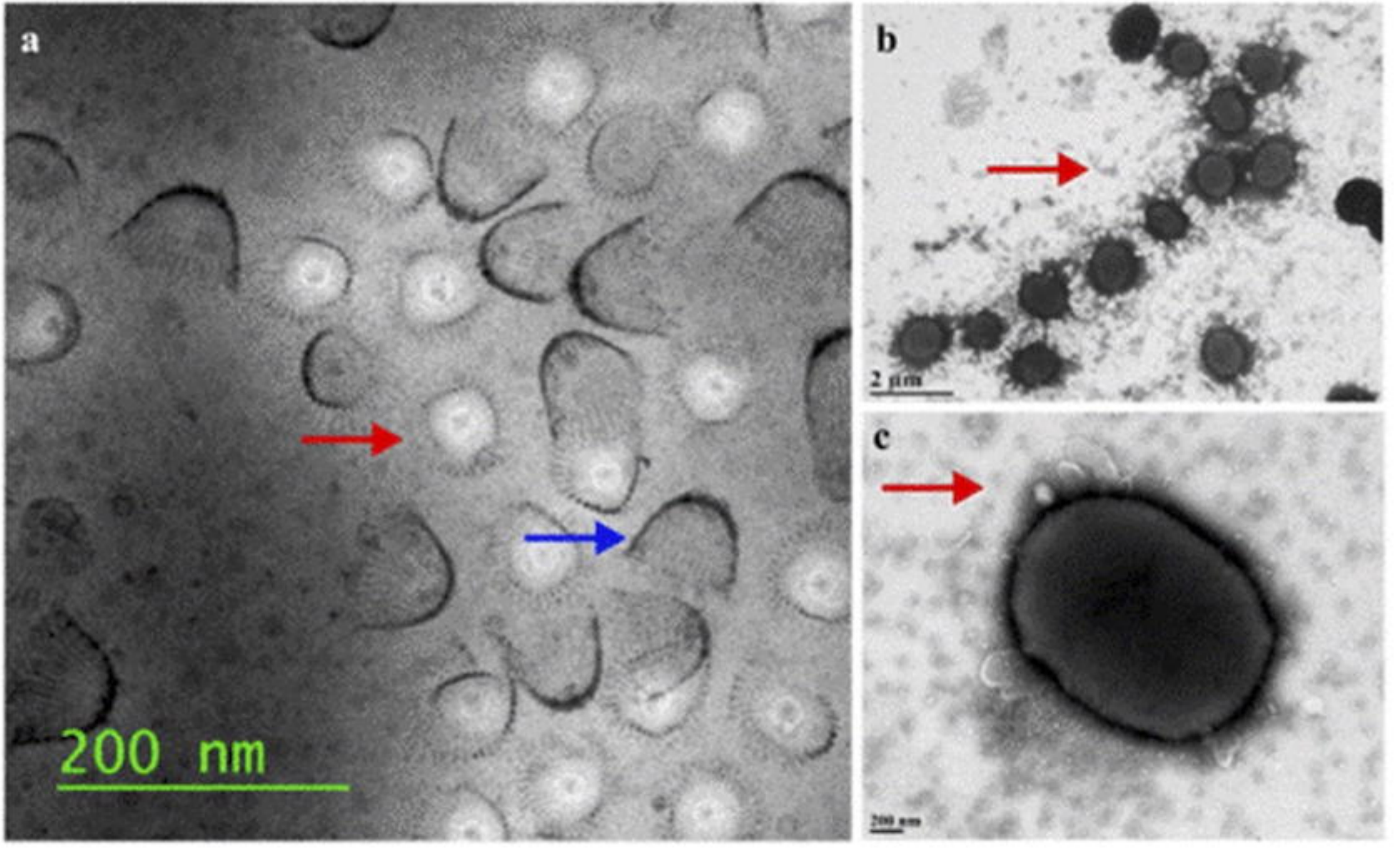
a
200 nm
b
2 µm
c
200 nm

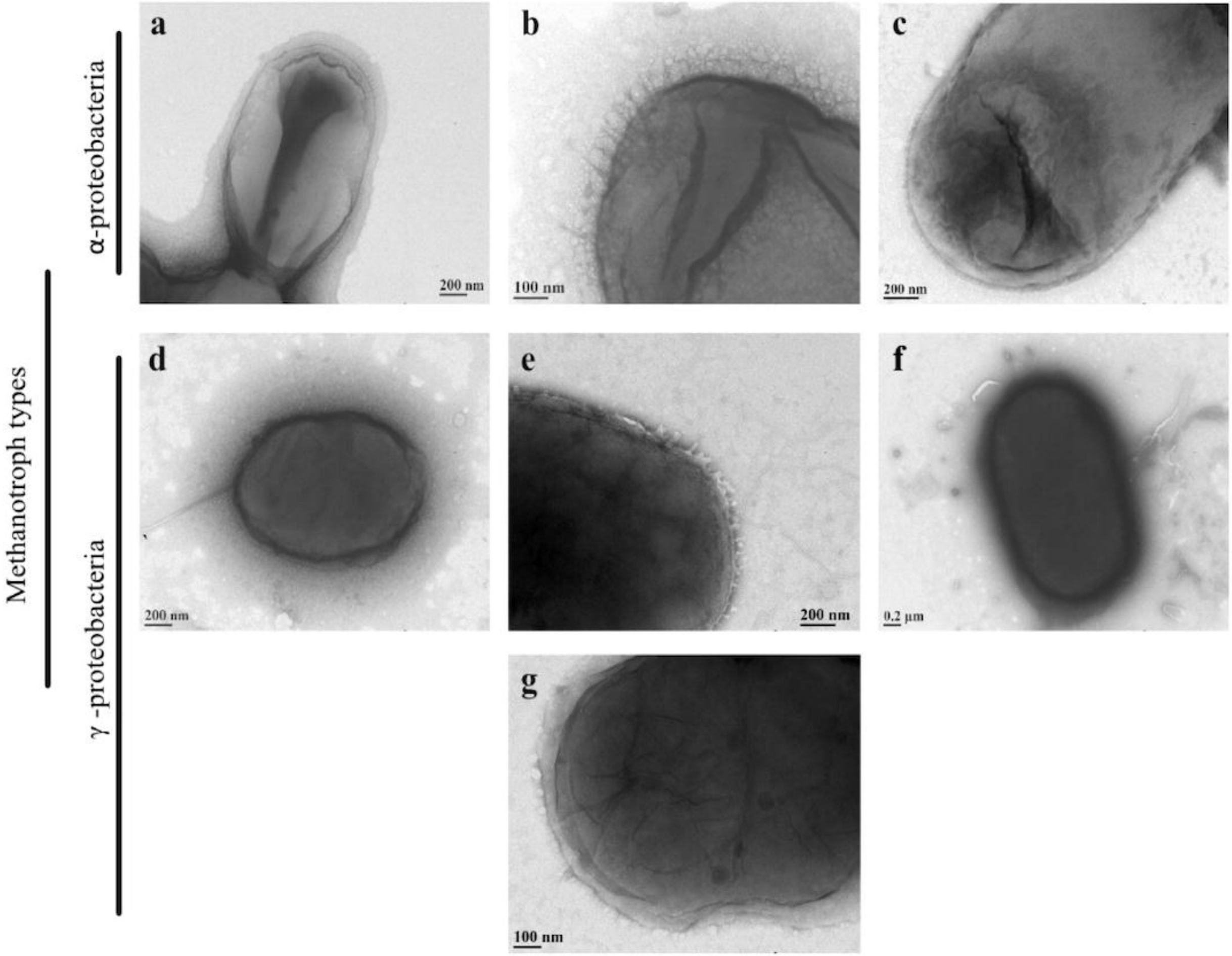
Methanotroph types
α-proteobacteria
γ -proteobacteria
a
200 nm
b
100 nm
c
200 nm
d
200 nm
e
200 nm
f
0.2 µm
g
100 nm

Methylomicrobium album BG8 (taxid:686340)				*Methylomonas denitrificans* FJG1 (taxid:1538553)				*Methylicorpusculum oleiharenae* XLMV4[T] (taxid:1338687)				*Methylotuvimicrobium buryatense* 5GB1 (taxid:675511)				*Methylococcus capsulatus* Bath (taxid:243233)			
GeneBank ID	Accession	Description	Length (aa)	Reference Sequence	Query Cov	E value	% Identity	Reference Sequence	Query Cov	E value	% Identity	Reference Sequence	Query Cov	E value	% Identity	Reference Sequence	Query Cov	E value	% Identity
EIC29550.1	H8GNF7	Flagellar hook protein FlgE	431	WP_036275189.1	100%	3.0E-150	52%	WP_159659411.1	100%	1.0E-139	51%	WP_017842460.1	100%	3.0E-143	51%	-	-	-	-
EIC29497.1	H8GMU5	Flagellin	761	WP_036276946.1	39%	9.0E-52	48%	WP_159652144.1	39%	8.0E-55	66%	WP_017842294.1	61%	1.0E-56	40%	-	-	-	-
EIC28933.1	H8GHU9	Prepilin-type N-terminal cleavage/methylation domain-containing protein	158	WP_036277617.1	25%	2.0E-10	55%	WP_331001651.1	49%	2.0E-21	56%	WP_017840688.1	91%	3.0E-26	39%	WP_010960785.1	85%	5.0E-25	42%
EIC28015.1	H8GKK7	Ca2+-binding protein, RTX toxin	1044	WP_062328457.1	31%	9.0E-12	29%	WP_159658860.1	30%	6.0E-15	27%	WP_017842713.1	89%	0.0E+00	47%	-	-	-	-
EIC31463.1	H8GIF1	Type 1 secretion C-terminal target domain protein	1392	WP_062328971.1	6%	8.0E-13	51%	WP_159658860.1	17%	4.0E-15	55%	WP_144053590.1	16%	8.0E-13	40%	-	-	-	-
EIC29232.1	H8GKR0	Uncharacterized protein	299	WP_036278985.1	99%	2.0E-74	42%	WP_159657453.1	99%	2.0E-75	44%	WP_017840936.1	87%	2.0E-80	46%	WP_010960992.1	97%	4.0E-41	32%
EIC28502.1	H8GPP0	Uncharacterized protein	118	WP_036273854.1	100%	7.0E-64	77%	WP_159658499.1	92%	3.0E-46	62%	-	-	-	-	-	-	-	-
EIC31556.1	H8GJ49	Outer membrane cobalamin receptor protein	691	WP_036276066.1	68%	1.0E-08	24%	WP_159657167.1	26%	3.0E-13	27%	WP_017840490.1	21%	5.0E-08	24%	WP_228370216.1	23%	5.0E-04	27%
EIC30073.1	H8GGW0	TonB-dependent siderophore receptor	787	WP_064044684.1	94%	6.0E-69	30%	WP_159658092.1	100%	0.0E+00	73%	WP_017841134.1	92%	4.0E-67	29%	AAU92033.1	23%	3.0E-15	29%
EIC31412.1	H8GIA0	ATP synthase epsilon chain	140	WP_033156953.1	99%	2.0E-73	81%	WP_159657005.1	100%	2.0E-53	84%	WP_026130213.1	100%	1.0E-53	84%	WP_010959386.1	97%	5.0E-35	67%
EIC30346.1	H8GJI6	LPS-assembly protein LptD	1003	WP_062329806.1	95%	0.0E+00	43%	WP_159657794.1	96%	0.0E+00	45%	WP_017842102.1	98%	0.0E+00	47%	WP_228370330.1	91%	0.0E+00	36%
EIC28701.1	H8GFV0	Type I secretion system ABC transporter, PrtD family*	570	WP_062329155.1	94%	3.0E-69	29%	MCD2450911.1	91%	4.0E-57	28%	WP_017842710.1	98%	0.0E+00	81%	WP_010960270.1	42%	1.0E-35	33%
EIC28702.1	H8GFV1	Type I secretion membrane fusion protein, HlyD family*	440	WP_062329159.1	100%	8.0E-39	28%	WP_159658692.1	95%	1.0E-27	26%	WP_017842711.1	100%	0.0E+00	70%	WP_218800424.1	10%	2.0E-03	37%
EIC28703.1	H8GFV2	Type I secretion outer membrane protein, TolC family	464	WP_036273387.1	91%	2.0E-50	30%	WP_231089141.1	92%	6.0E-44	28%	WP_138767192.1	98%	0.0E+00	62%	WP_010960559.1	95%	7.0E-35	28%
EIC28704.1	H8GFV3	S-layer protein	4036	WP_062328457.1	4%	2.0E-03	29%	WP_159658860.1	4%	1.1E-02	29%	WP_017842715.1	44%	1.0E-57	32%	-	-	-	-
EIC29875.1	H8GR48	Type I secretion outer membrane protein, TolC family*	469	WP_036273387.1	92%	1.0E-151	53%	WP_231089141.1	92%	2.0E-180	60%	WP_017840392.1	94%	0.0E+00	63%	WP_010960559.1	91%	3.0E-98	44%
EIC30282.1	H8GIU2	Type I secretion system ATPase, LssB family*	724	WP_062329155.1	97%	0.0E+00	73%	WP_159658693.1	97%	3.0E-100	31%	WP_017841836.1	97%	0.0E+00	63%	WP_017364746.1	40%	4.0E-56	40%
EIC30283.1	H8GIU3	Type I secretion membrane fusion protein, HlyD family*	453	PPD37447.1	100%	0.0E+00	69%	WP_159658692.1	97%	2.0E-42	27%	WP_014150105.1	98%	0.0E+00	58%	WP_017364682.1	28%	1.0E-09	34%
EIC30284.1	H8GIU4	Response regulator containing a CheY-like receiver domain and an HTH DNA-binding domain*	213	WP_278209298.1	99%	7.0E-51	47%	WP_159659411.1	97%	2.0E-46	38%	WP_017839778.1	99%	2.0E-56	42%	-	-	-	-
EIC30285.1	H8GIU5	Dihydropteroate synthase*	275	MFM8342556.1	96%	5.0E-136	70%	WP_159653036.1	96%	5.0E-115	65%	WP_017839219.1	96%	5.0E-115	65%	WP_198323910.1	97%	5.0E-121	66%

Methane Methanol

A

B

C

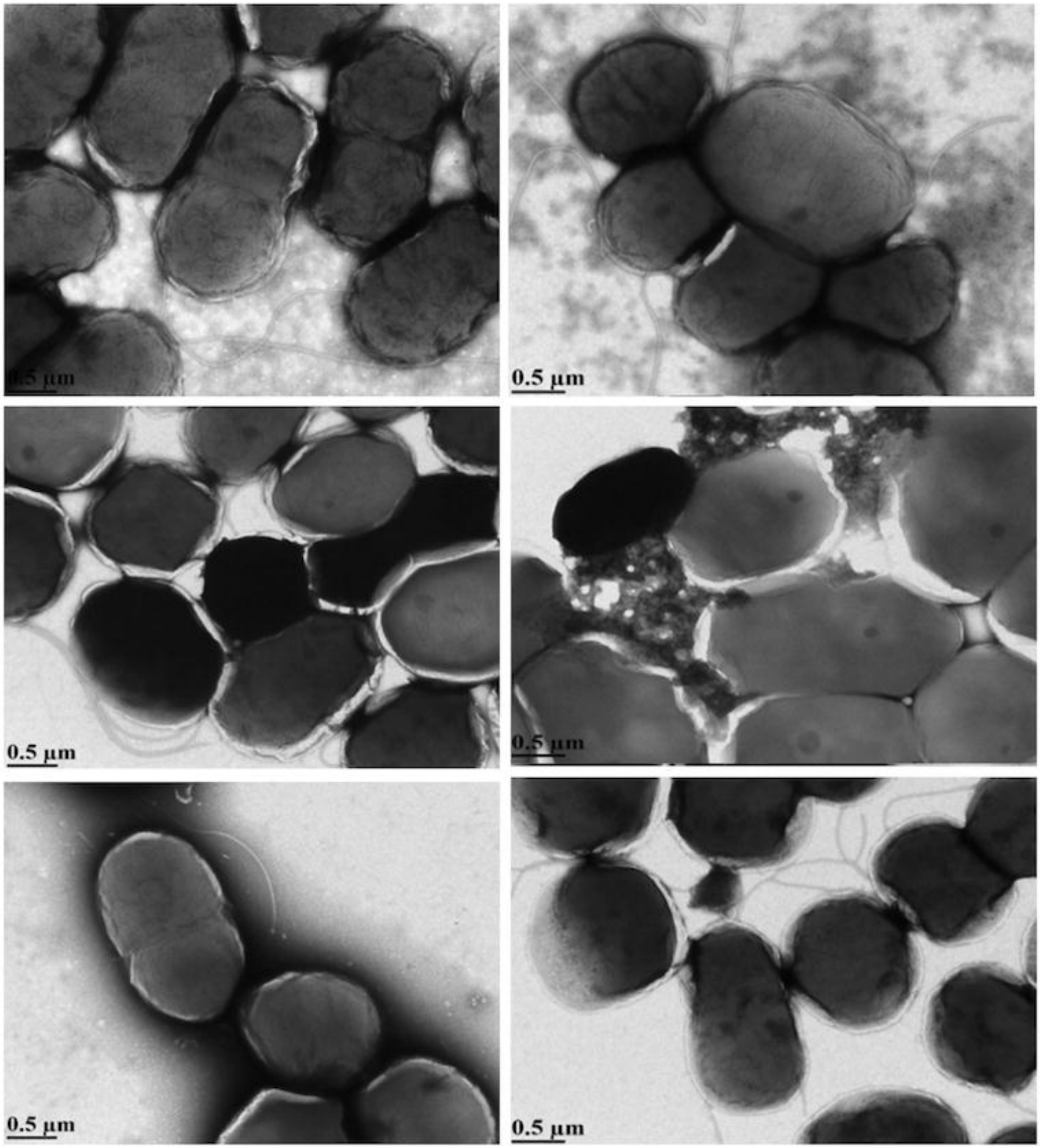

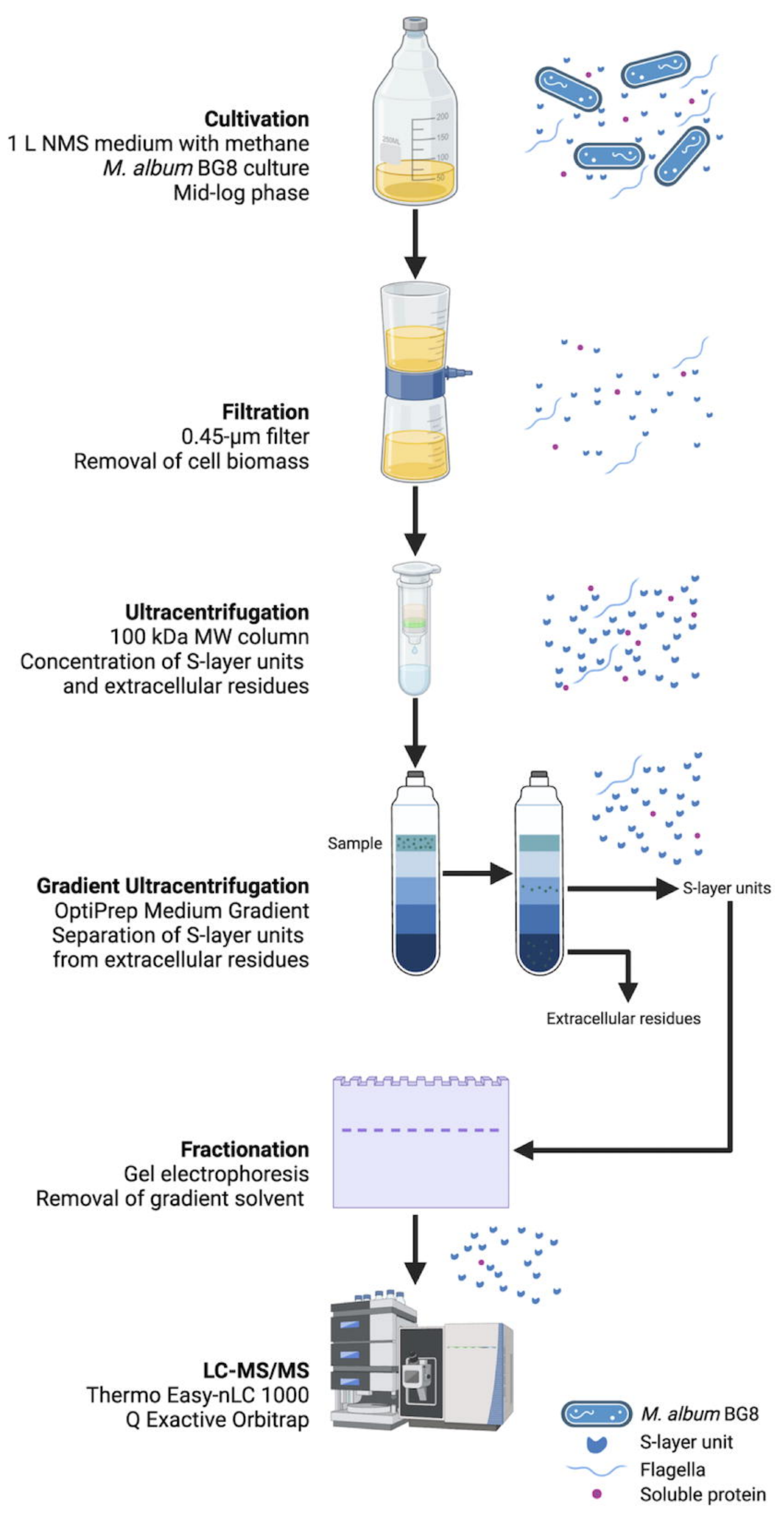
Cultivation
1 L NMS medium with methane
M. album BG8 culture
Mid-log phase
Filtration
0.45-µm filter
Removal of cell biomass
Ultracentrifugation
100 kDa MW column
Concentration of S-layer units
and extracellular residues
Gradient Ultracentrifugation
OptiPrep Medium Gradient
Separation of S-layer units
from extracellular residues
Sample
S-layer units
Extracellular residues
Fractionation
Gel electrophoresis
Removal of gradient solvent
LC-MS/MS
Thermo Easy-nLC 1000
Q Exactive Orbitrap
M. album BG8
S-layer unit
Flagella
Soluble protein